Supplementary Information

Complex Interactions Between Genes Controlling Trafficking in Primary Cilia

Polloneal Jymmiel R. Ocbina[1,2,6], Jonathan T. Eggenschwiler[3], Ivan Moskowitz[4,5] and Kathryn V. Anderson[1,7]

[1] Developmental Biology Program, Sloan-Kettering Institute 1275 York Avenue New York, NY 10065

[2] Neuroscience Program, Weill Graduate School of Medical Sciences, Cornell University 445 East 69th Street New York, NY 10065

[3] Department of Molecular Biology, Princeton University, Princeton, NJ 08544

[4] Department of Pediatrics, The University of Chicago, Chicago, IL, 60637, USA

[5] Department of Pathology, The University of Chicago, Chicago, IL, 60637, USA

[6] Current address: Department of Genetics, Yale University School of Medicine, New Haven, CT 06510

[7] Corresponding author: k-anderson@sloankettering.edu

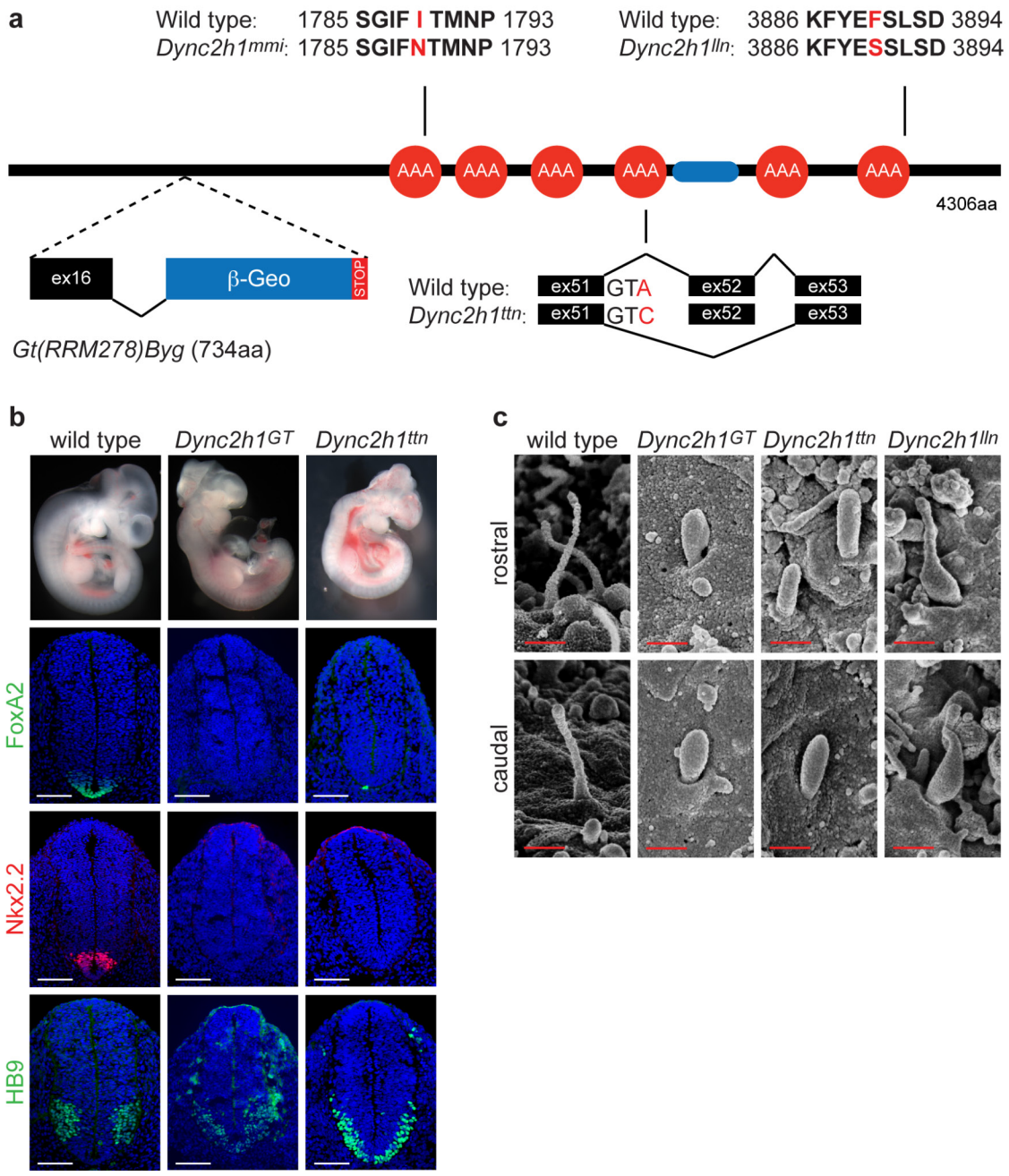

Supplementary Figure 1. Mutations in *Dync2h1* disrupt cilia morphology and Shh-dependent neural patterning. (**a**) The motor domain of cytoplasmic dynein-2 heavy chain (Dync2h1) protein includes six AAA-ATPase domains (red) and a microtubule binding domain (blue). The ENU-induced *ling-ling* (*lln*), *tian-tian (ttn)*, and *mei-mei* (*mmi*) alleles identified in our screens disrupt the motor domain of Dync2h1, and the gene-trap allele *Gt(RRM278)Byg* inserts in the N-terminal tail domain and is a protein-null allele (not shown). (**b**), Similar to *lln* mutants, both *ttn* and *Gt(RRM278)Byg* mutants lack Shh-dependent cell types in the E10.5 neural tube. Floor plate (FoxA2, green) and V3 progenitor (Nkx2.2, red) domains are not specified and motor neurons (HB9, green) are present only in the caudal neural tube; dorsal up. (**c**), Scanning electron micrographs show that neural tube primary cilia in *Dync2h1* mutants are bloated; dimensions are given in **Supplementary Table1**. Scale bars represents 100 μm (**b**) 500 nm (**c**).

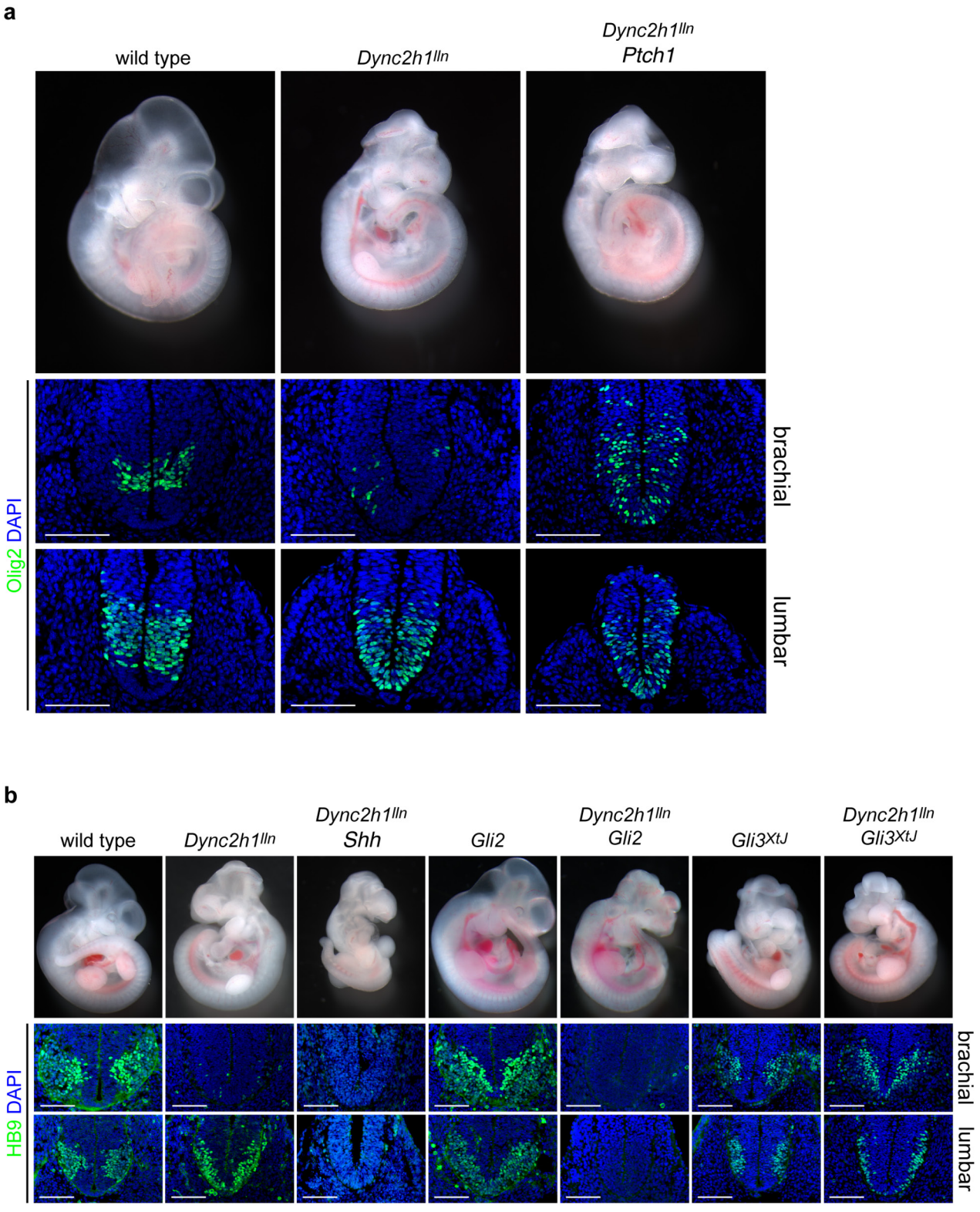

Ocbina, *et al.*, Supplementary Figure 2

Supplementary Figure 2. Dync2h1 acts downstream of Patched1 and upstream of the Gli transcription factors. (**a**), *Patched1* (*Ptch1*), which encodes the membrane receptor for Shh, is a negative regulator of the pathway. *Ptch1*$^{-/-}$ mutants and the embryos have a completely ventralized neural tube [48], whereas *Dync2h1*$^{lln/lln}$ *Ptch1*$^{-/-}$ double mutants, like *Dync2h1*$^{lln/lln}$ mutants, lack the most ventral neural cell types that depend on high levels of Shh pathway activity, the floor plate and V3 progenitors. As in *Dync2h1*$^{lln/lln}$ single mutants, motor neurons were specified in the caudal neural tube of *Dync2h1*$^{lln/lln}$ *Ptch1*$^{-/-}$ double mutants. Because removal of *Ptch1* in the absence of dynein cannot activate the pathway to high levels, *Dync2h1* acts downstream of *Ptch1*. (**b**), Motor neurons were not specified at any rostrocaudal level of *Dync2h1*$^{lln/lln}$ *Shh*$^{-/-}$ double mutant embryos, demonstrating that specification of motor neurons in the caudal neural tube of *Dync2h1*$^{lln/lln}$ mutants is Shh-dependent. Motor neurons were not specified at any rostrocaudal position in *Dync2h1*$^{lln/lln}$ *Gli2*$^{-/-}$ double mutants, showing that the motor neurons specified in *Dync2h1*$^{lln/lln}$ embryos depend on the Hh pathway mediator Gli2. Gli3 acts mainly as a transcriptional repressor in the neural tube and motor neurons, which were not present in the brachial neural tube of *Dync2h1*$^{lln/lln}$ mutants, were specified in *Dync2h1*$^{lln/lln}$ *Gli3*$^{XtJ/XtJ}$ double mutants, as in IFT-B *Gli3* double mutants [16]. Thus Dync2h1 acts at the same position in the pathway as IFT-B mutants, but there is a low level of response to Shh in the absence of *Dync2h1* that depends on the activity of Gli2. Scale bars represent 100 μm (**a**) and (**b**).

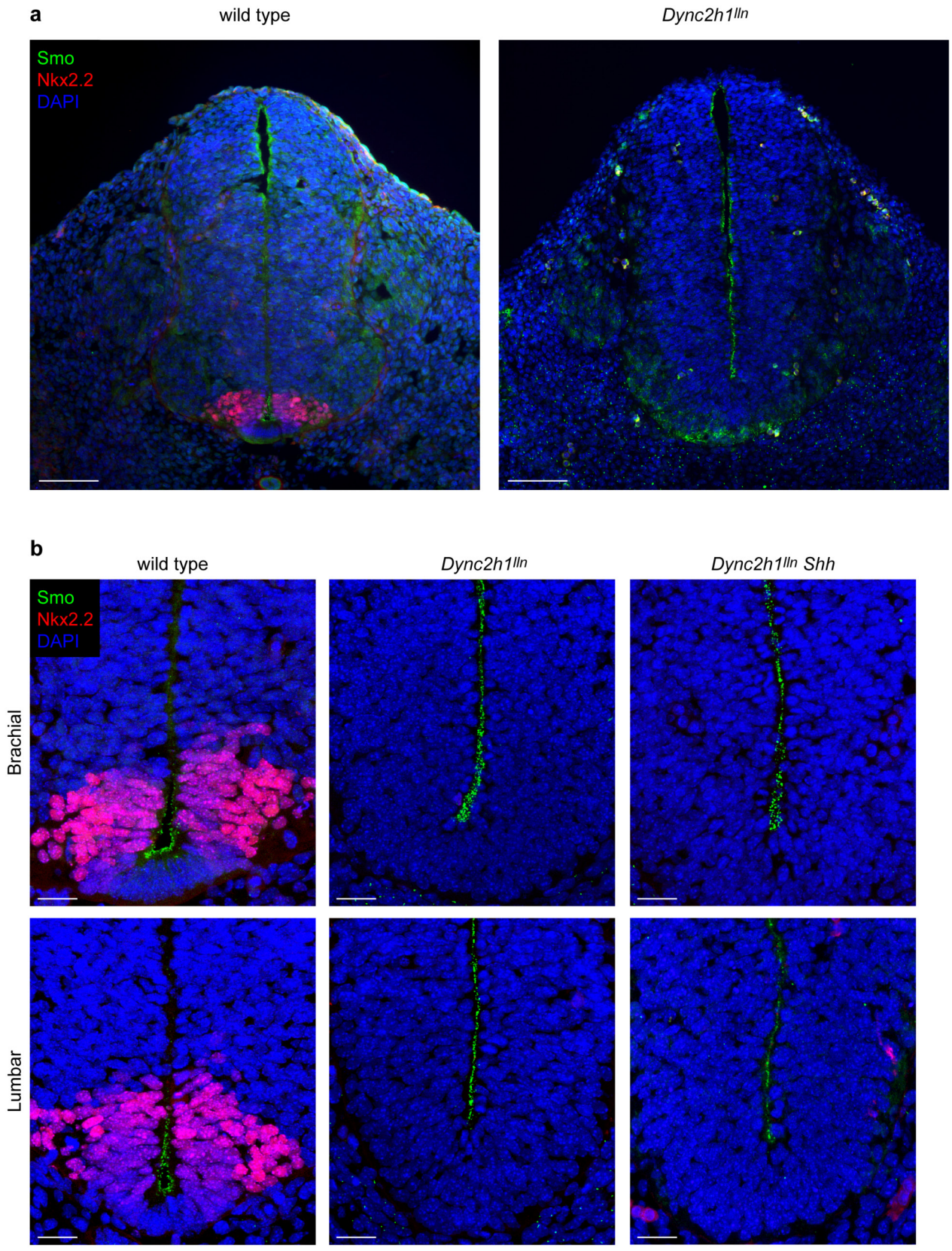

Ocbina, *et al.*, Supplementary Figure 3

Supplementary Figure 3. **Accumulation of Smo in *Dync2h1^{lln}* mutants is independent of Shh.** (**a**), Low magnification views of wild type and *Dync2h1$^{lln/lln}$* neural tubes at the brachial level showing Smo (green) localization in the rostral neural tube. Localization of Smo is ventrally-restricted in wild-type embryos, but is present throughout the neural tube in *Dync2h1$^{lln/lln}$* mutants. (**b**), Smo (green) localization in wild type (left panels), *Dync2h1$^{lln/lln}$* (middle panels) and *Dync2h1$^{lln/lln}$ Shh$^{-/-}$* embryos. Nkx2.2 (red) marks the position of V3 progenitors at E10.5 at both brachial (top) and lumbar (bottom) levels. Even in the absence of Shh (*Dync2h1$^{lln/lln}$ Shh$^{-/-}$* mutants), Smo accumulates to high levels in the cilia when Dync2h1 function is absent. Dorsal is up. Scale bars represent 100 μm (**a**) and 25 μm (**b**).

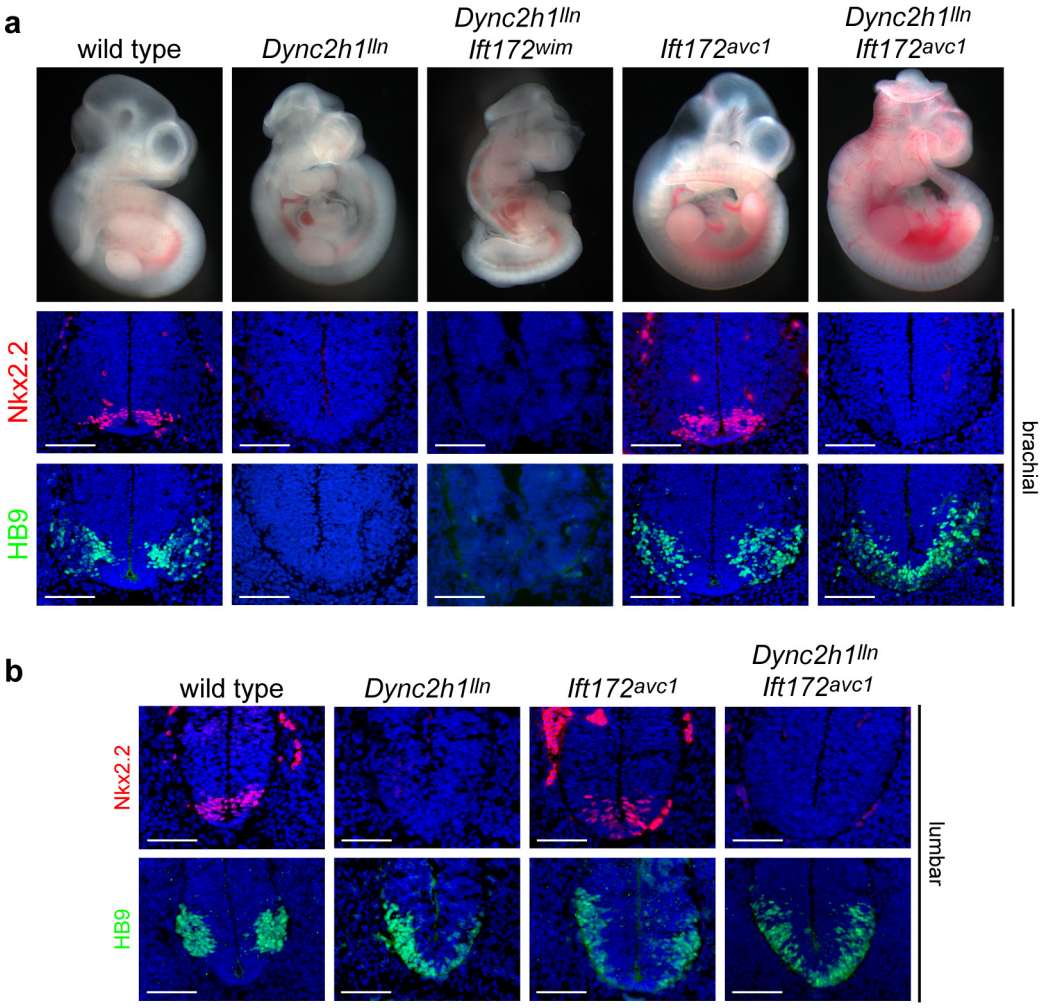

Supplementary Figure 4. **Neural patterning in the caudal neural tube of *Dync2h1^{lln} Ift172^{avc1}* mutants.** Neural tube patterning in the caudal neural tube of *Dync2h1$^{lln/lln}$ Ift172$^{avc1/avc1}$* double mutants is indistinguishable from patterning in *Dync2h1$^{lln/lln}$* mutants, which specify motor neurons (HB9, green), but not V3 progenitors (Nkx2.2, red). Dorsal is up. Scale bars represent 100 μm (**a**) and (**b**).

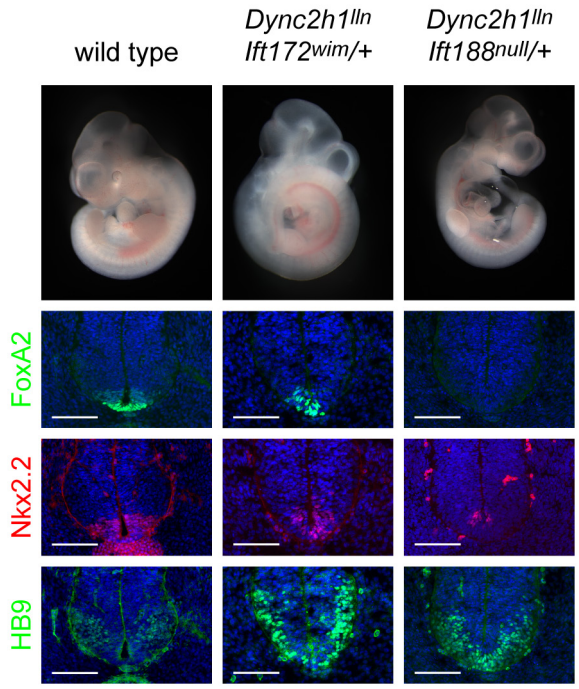

Supplementary Figure 5. Decreased activity of IFT-B rescues ventral cell fates in *Dync2h1^{lln}* mutants. Heterozygosity for null alleles of either *Ift172* (*wim*) or *Ift88* (*null*) partially rescues Shh-dependent ventral neural fates in *Dync2h1$^{lln/lln}$* mutants at E10.5. Ventral cell fates such as the floor plate (FoxA2, green) and p3 (Nkx2.2, red) are specified in the caudal neural tube of *Dync2h1$^{lln/lln}$ Ift172^{wim}*/+ mutants, although the dorsal and ventral boundaries of these domains are less well-defined than in *Dync2h1$^{lln/lln}$ Ift172^{avc1}*/+ mutants. For example, floor plate and V3 progenitors are mixed and both occupy the ventral midline, and the motor neuron domain is ventrally expanded and is only slightly separated at the midline in *Dync2h1$^{lln/lln}$ Ift172^{wim}*/+ mutants. A similar partial rescue was observed in *Dync2h1$^{lln/lln}$ Ift88^{null}*/+ mutants, although floor plate cells (FoxA2) were not specified. Scale bars represent 100 μm.

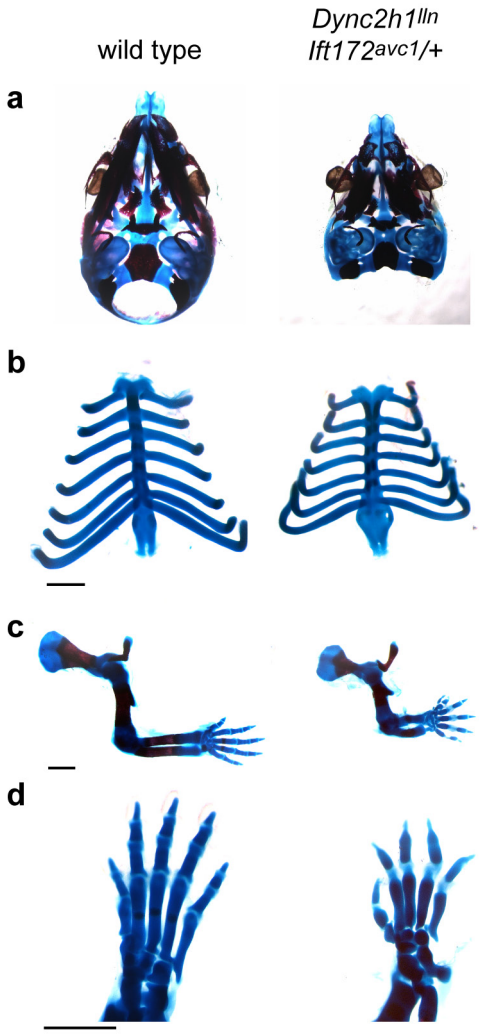

Supplementary Figure 6. *Dync2h1*$^{lln/lln}$ *Ift172*^{avc1}/+ mutants display additional phenotypes at E16.5. (**a**) Ventral view of E16.5 skull showing incomplete closure of the base of the cranium. (**b**) *Dync2h1*$^{lln/lln}$ *Ift172*^{avc1}/+ mutants show a slight shortening of the sternum (n=4/5). (**c**) E16.5 right forelimbs showing shortening of the long bones (n=2/5). (**d**) Compared with the forelimbs (**Fig. 4c**) a total of 2/10 *Dync2h1*$^{lln/lln}$ *Ift172*^{avc1}/+ mutant hindlimbs were polydactylous. Shown here is a non-polydactylous *Dync2h1*$^{lln/lln}$ *Ift172*^{avc1}/+ mutant right hindlimb. All scale bars are 1mm.

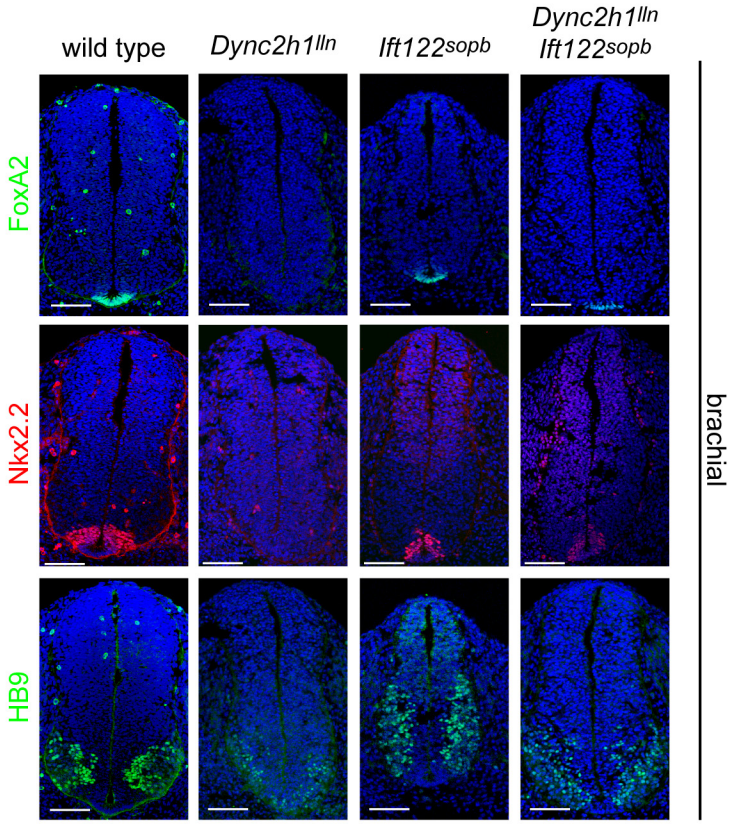

Supplementary Figure 7. Neural patterning in the rostral neural tube of *Dync2h1^{lln} Ift122^{sopb}* mutants. All ventral neural cell fates are specified in the rostral neural tube of *Dync2h1$^{lln/lln}$ Ift122$^{sopb/sopb}$* mutants, including the floor plate (FoxA2, green) and V3 progenitors (Nkx2.2, red) that are absent in *Dync2h1$^{lln/lln}$* single mutants. Dorsal is up. Scale bars represent 100 μm.

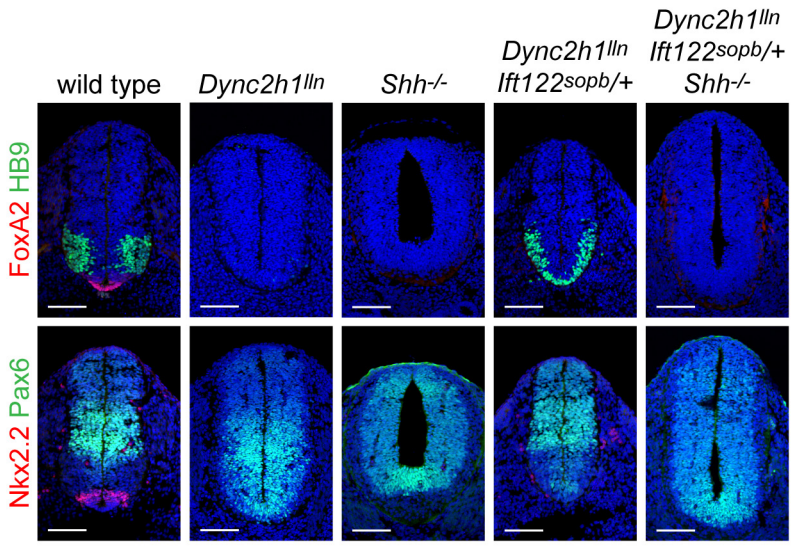

Supplementary Figure 8. Shh responsiveness in the brachial neural tube of *Dync2h1$^{lln/lln}$ Ift122^{sopb}*/+ embryos. Motor neurons (HB9, green, middle panels) were partially rescued in the rostral neural tube of *Dync2h1$^{lln/lln}$ Ift122^{sopb}*/+ mutant embryos but were absent in *Dync2h1$^{lln/lln}$ Ift122^{sopb}*/+ *Shh$^{-/-}$* embryos. Unlike the lumbar neural tube (**Fig. 6**), few floor plate cells (FoxA2, red, middle panels) and V3 progenitors (Nkx2.2, red, bottom panels) were rescued at brachial levels. The Pax6 domain (green, bottom panels), which is restricted by low levels of Shh signaling, was ventrally expanded in *Shh$^{-/-}$* and *Dync2h1$^{lln/lln}$ Ift122^{sopb}*/+ *Shh$^{-/-}$* embryos. Scale bars represent 100 μm.

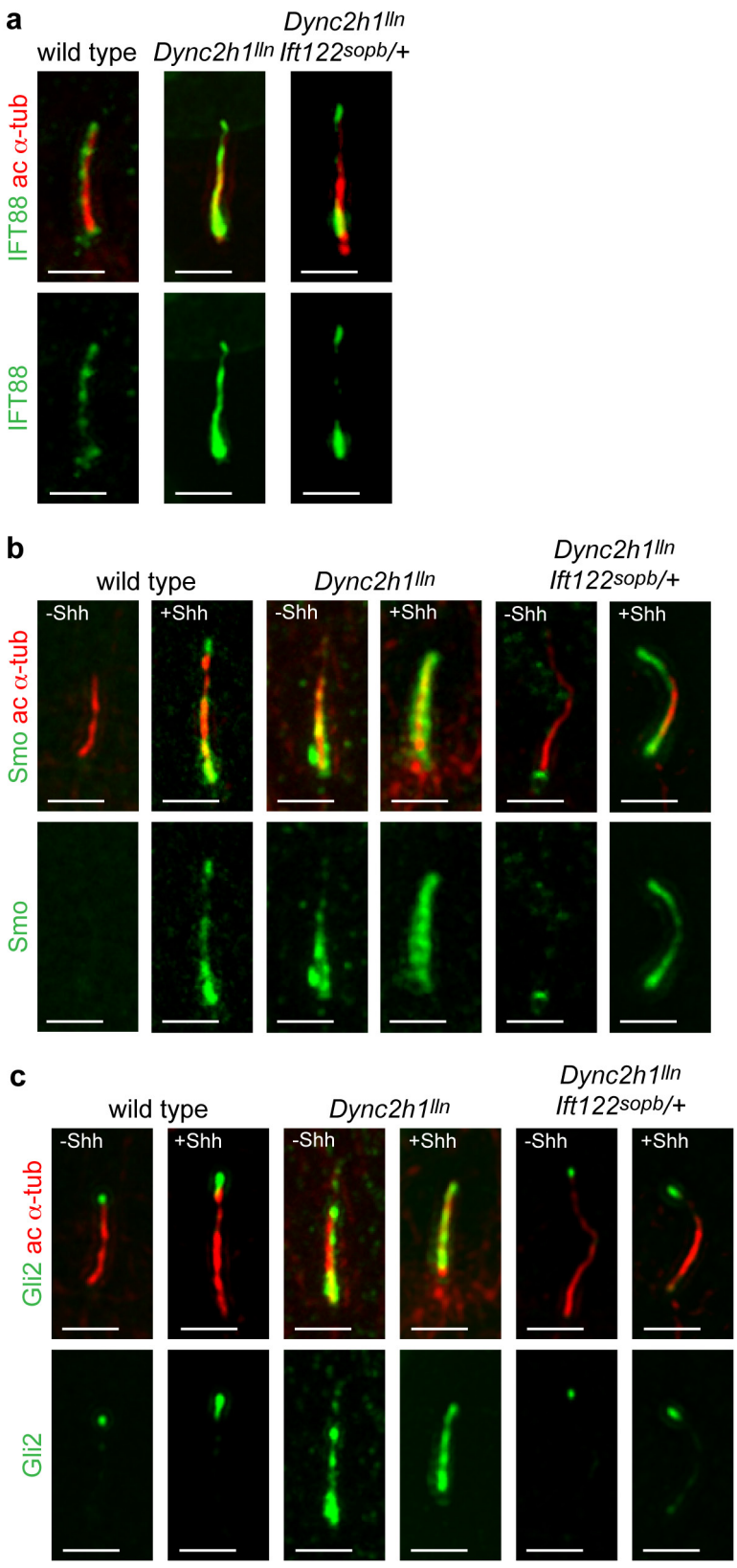

Ocbina, *et al.*, Supplementary Figure 9

Supplementary Figure 9. Cilia localization of IFT88, Smo and Gli2 in *Dync2h1*$^{lln/lln}$ *Ift122*^{sopb}/+ cilia. IFT88 (a, green), Smo (b, green) and Gli2 (c, green) in cilia (acetylated α-tubulin, red) are localized normally in *Dync2h1*$^{lln/lln}$ *Ift122*^{sopb}/+ mutants. Images are identical to (**Fig. 6b, c and d)** with single channel data for IFT88, Smo and Gli2 shown for clarity. Scale bars represent 500 nm.

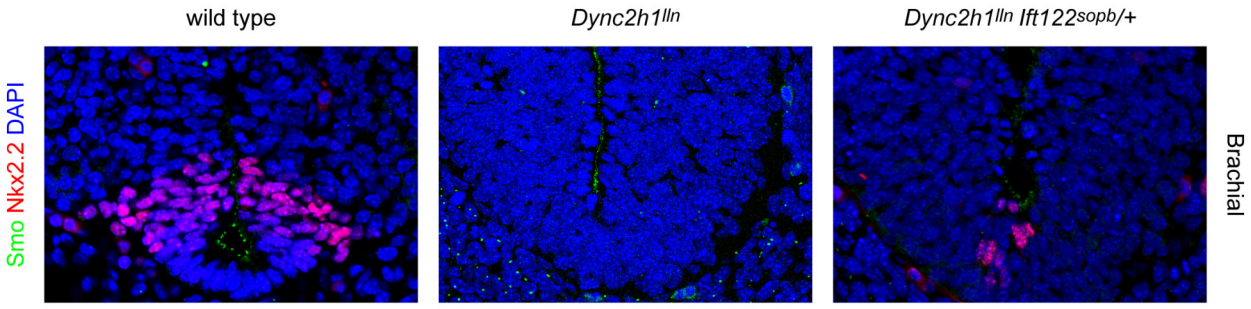

Supplementary Figure 10. Smo localization in the neural tube is rescued in *Dync2h1$^{lln/lln}$ Ift122^{sopb}*/+ mutants. Smo (green) localization in neural tube sections of wild type (left panel), *Dync2h1$^{lln/lln}$* (middle panel) and *Dync2h1$^{lln/lln}$ Ift122^{sopb}*/+ embryos at the brachial level. Nkx2.2 (red) expression marks the position of V3 progenitors. Compared with *Dync2h1$^{lln/lln}$* mutants where Smo accumulates in cilia throughout the neural tube, Smo is restricted to the cilia in the ventral neural tube of *Dync2h1$^{lln/lln}$ Ift122^{sopb}*/+ embryos where a few V3 progenitors are specified.

Supplementary Table 1. Neural primary cilia length

	Length (nm)			Width (nm)			n
wild type	960 ± 289		NS	178 ± 20		***	642
Dync2h1$^{lln/lln}$	875 ± 327	NS		314 ± 30	***		600
Dync2h1$^{ttn/ttn}$	728 ± 190	***	***	337 ± 47	***	***	146
Dync2h1$^{Gt(RRM278)Byg}$	658 ± 176	***	***	347 ± 54	***	***	72
Ift172$^{avc1/avc1}$	682 ± 225	***	***	171 ± 50	NS	***	81
Dync2h1$^{lln/lln}$; *Ift172*^{avc1}/+	1219 ± 343	***	***	241 ± 71	***	***	235
Dync2h1$^{lln/lln}$; *Ift172*$^{avc1/avc1}$	399 ± 214	***	***	179 ± 27	NS	***	235
Ift122$^{sopb/sopb}$	704 ± 259	***	***	240 ± 37	***	***	164
Dync2h1$^{lln/lln}$; *Ift122*^{sopb}/+	1229 ± 437	***	***	240 ± 30	***	***	235
Dync2h1$^{lln/lln}$; *Ift122*$^{sopb/sopb}$	448 ± 189	***	***	216 ± 48	***	***	399

Measurement of primary cilia in the developing spinal cord. Data represent mean values ± S.D. Asterisks denote statistical significance between values obtained for the specified genotype and wild type (red) or *Dync2h1*^{lln} (blue) values analyzed using one-way ANOVA followed by a post hoc Tukey test. NS, not significant; *, $P \leq 0.05$; **, $P \leq 0.01$; ***, $P \leq 0.001$.

Supplementary Table 2. Quantitation of ciliary IFT88

	IFT88 (a.u.)			n
wild type	100 ± 7.42		***	38
Dync2h1$^{lln/lln}$	230 ± 9.73	***		102
Ift172$^{avc1/avc1}$	47 ± 3.15	*	***	33
Dync2h1$^{lln/lln}$; *Ift172*^{avc1}/+	125 ± 6.20	NS	***	136
Dync2h1$^{lln/lln}$; *Ift172*$^{avc1/avc1}$	55 ± 3.41	NS	***	34
Ift122$^{sopb/sopb}$	97 ± 4.22	NS	***	114
Dync2h1$^{lln/lln}$; *Ift122*^{sopb}/+	153 ± 5.48	**	***	152
Dync2h1$^{lln/lln}$; *Ift122*$^{sopb/sopb}$	69 ± 6.02	NS	***	78

Measurement of IFT88 protein accumulation in primary cilia of MEFs derived from wild-type and mutant embryos. Data represent means values (± S.D.) of the relative fluorescence intensity of IFT88 staining in cells averaged over three independent experiments. Asterisks denote statistical significance between values obtained for the specified genotype and wild type (red) or *Dync2h1*^{lln} (blue) values analyzed using one-way ANOVA followed by a post hoc Tukey test. NS, not significant; *, $P \leq 0.05$; **, $P \leq 0.01$; ***, $P \leq 0.001$.

Supplementary Table 3. Gli2 Cilia Accumulation

	no Shh (a.u.)			n	with Shh (a.u.)			n
wild type	1680 ± 493		***	115	6688 ± 2860		***	58
Dync2h1$^{lln/lln}$	10270 ± 4151	***		81	12088 ± 9280	***		37
Ift172$^{avc1/avc1}$	848 ± 744	NS	***	56	3987 ± 2048	*	***	47
Dync2h1$^{lln/lln}$; *Ift172*^{avc1}/+	1185 ± 1469	NS	***	86	6724 ± 5177	NS	***	89
Dync2h1$^{lln/lln}$; *Ift172*$^{avc1/avc1}$	2764 ± 1567	NS	***	52	4078 ± 2817	NS	***	47
Ift122$^{sopb/sopb}$	6349 ± 2796	*	**	20	6001 ± 2613	NS	***	54
Dync2h1$^{lln/lln}$; *Ift122*^{sopb}/+	1454 ± 1024	NS	***	77	4274 ± 2635	***	***	53
Dync2h1$^{lln/lln}$; *Ift122*$^{sopb/sopb}$	4459 ± 2925	NS	***	48	6107 ± 3018	***	***	53

Measurement of Gli2 protein accumulation in primary cilia of MEFs derived from wild-type and mutant embryos before and after treatment with Shh conditioned media. Data represent means values (± S.D.) of the relative fluorescence intensity of Gli2 staining in cells averaged over three independent experiments. Asterisks denote statistical significance between values obtained for the specified genotype and wild type (red) or *Dync2h1*^{lln} (blue) values analyzed using one-way ANOVA followed by a post hoc Tukey test. NS, not significant; *, $P \leq 0.05$; **, $P \leq 0.01$; ***, $P \leq 0.001$.

Supplementary Table 4. Oligonucleotide Sequences

Primers	Sequence
wmp-G1 F	5’ GCGGCCATCAACCACTATATTGACACC 3’
wmp-G1 R	5’ GCACAGCCAGGAAGAACATT 3’
sopb-G1 F	5’ GGTAGCGCAGGTAGCTGAAG 3’
sopb-G1 R	5’ TTCCATTGGGAAGTTGAAGG 3’